Pump-to-mode size ratio dependence of thermal loading in diode-end-pumped solid-state lasers

Yung-Fu Chen

Department of Electrophysics, National Chiao Tung University, Hsinchu, Taiwan

Received February 29, 2000; revised manuscript received July 5, 2000

The fractional thermal loading in a diode-end-pumped solid-state laser is deduced from experimental measurement of the critical pump power. The results show that fractional thermal loading critically depends on the pump-to-mode size ratio. This dependence is attributed to the effect of the pump-to-mode size ratio on the population inversion and to the effect of energy-transfer upconversion. Rigorous modeling calculations have been performed to yield a comprehensive understanding of the thermal loading in diode-end-pumped solid-state lasers. © 2000 Optical Society of America [S0740-3224(00)01011-0]

OCIS codes: 140.3480, 140.3580, 140.6810.

1. INTRODUCTION

An end-pumped configuration in solid-state lasers offers the possibility of achieving high conversion efficiencies for fundamental mode operation. Power scaling of diode-end-pumped solid-state lasers is usually impeded by the thermal effect that results from the small volume of the pumping profile. One of the most important parameters that quantitatively characterize the strength of thermal effects is fractional thermal loading ξ, defined as the ratio of the thermal energy generated in the gain medium to the absorbed pump energy. The thermal loading leads to a lensing behavior in the gain medium. The thermally induced lensing effect is a critical factor for resonator design. Therefore, thermal loading needs to be thoroughly understood and characterized for optimization of the resonator design.

Several approaches,[1–6] including calorimetric,[4] interferometric,[5] and mode-degeneration methods,[6] have been proposed for measuring thermal lensing or thermal loading in end-pumped solid-state lasers. Recently Chen and Kuo[7] used the thermally induced depolarization of the second-harmonic output to measure the fractional thermal loading under lasing conditions.

Here a method of measuring the fractional thermal loading in diode-end-pumped solid-state lasers under lasing conditions is presented. The experimental result reveals that the fractional thermal loading apparently increases with increasing pump-to-mode size ratio. This tendency is contrary to the prediction of the model developed by Hardman *et al.*,[8] who studied the influence of energy-transfer upconversion (ETU) on thermal loading with the assumption that the inversion population density is correlated to the critical inversion density at the threshold condition. To obtain a general, comprehensive understanding of the thermal loading in end-pumped lasers, the present author has analyzed the inversion population density by including ETU effects in the space-dependent rate-equation model. This analysis shows that the inversion population is evidently not correlated to the value at the threshold in an end-pumped laser, and this result, associated with the ETU effect, leads to the increase of thermal loading for a larger pump-to mode size ratio.

2. DETERMINATION OF THERMAL LOADING

The thermal lens of a laser crystal always affects the stability of a resonator. For a laser that is end pumped by a fiber-coupled diode, the focal length of the thermal lens, f_{th}, is given by[9,10]

$$\frac{1}{f_{\mathrm{th}}} = \frac{\xi P_{\mathrm{abs}}}{2\pi K_c \omega_p{}^2}\left[\mathrm{d}n_o/\mathrm{d}T + (n_o - 1)(1 + \nu)\alpha_T + n_o{}^3\alpha_T C_r\right], \quad (1)$$

where ξ is the fractional thermal loading, P_{abs} is the absorbed pump power, K_c is the thermal conductivity, n_o is the refractive index of the laser crystal, $\mathrm{d}n_o/\mathrm{d}T$ is the thermal-optic coefficient of n_o, ν is Poisson's ratio, α_T is the thermal expansion coefficient, C_r is the photoelastic coefficient, and ω_p is the average pump size in the active medium. Note that we derive Eq. (1) by including the effect of the temperature gradient across the entire crystal under conditions of conventional edge cooling.

For the linear cavity shown in Fig. 1 there exists a critical pump power P_{critical} at which the thermally induced lens will cause the laser cavity to be unstable. From the standard *ABCD* matrix approach, the critical thermal lens that corresponds to the critical pump power is given by[11]

$$\left(\frac{1}{f_{\mathrm{th}}}\right)_{\mathrm{critical}} = \frac{1}{d_2{}^*} - \frac{1}{\rho_1 - d_1}, \quad (2)$$

$$d_2{}^* = d_2 + l(1/n_o - 1), \quad (3)$$

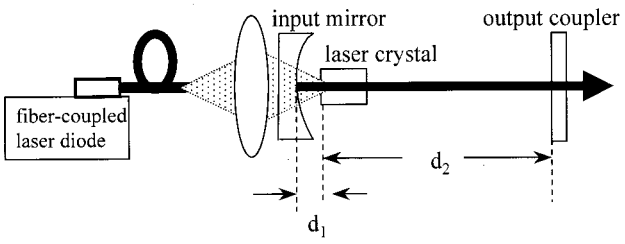

Fig. 1. Experimental setup for measuring thermal loading.

where ρ_1 is the radius of curvature of the input mirror, d_1 and d_2 are the distances between the mirrors and the incident end of the laser crystal, and l is the length of the laser crystal.

From Eqs. (1) and (2), the relationship between the fractional thermal loading and the critical pump power is given by

$$\xi = \frac{1}{P_{\text{critical}}}\left(\frac{1}{d_2{}^*} - \frac{1}{\rho_1 - d_1}\right) \times \frac{2\pi K_c \omega_p{}^2}{dn_o/dT + (n_o - 1)(1 + \nu)\alpha_T + n_o{}^3\alpha_T C_r}. \quad (4)$$

Equation (4) indicates that, as the critical pump power is determined, the fractional thermal loading can be obtained with the parameters of the laser system. Based on this fact, we measured the critical pump power from the input–output characteristic of the cavity with a 1.0-at.% Nd:YAG crystal and with an output coupler of $R = 85\%$ for several pump-to-mode size ratios ω_p/ω_o, where ω_o is the cavity mode size. The results are shown in Fig. 2, where the arrows represent the critical pump powers. Equation (4) reveals that, if the fractional thermal loading is independent of the pump size, the critical pump power is proportional to the square of the pump size. However, from Fig. 2 it can be seen that enhancement of the critical pump is not significant when the pump-to-mode size ratio increases from $\omega_p/\omega_o = 1.3$ to $\omega_p/\omega_o = 1.6$. This result implies that the fractional thermal loading should depend on the pump-to-mode size ratio.

With the measured critical pump power and from Eq. (4) with the values of the parameters in the present cavity, the deduced fractional thermal loading is shown in Fig. 3 for several pump-to-mode size ratios. To extract the fractional thermal loading with good precision we require knowing the quantities for the thermal and thermal-optical parameters. Several values have been found in the literature for a Nd:YAG crystal. The value 0.12 W K^{-1} cm^{-1} for the thermal conductivity is averaged from the values 0.14,[12] 0.13,[13–15] 0.129,[16] and 0.105.[17] Room-temperature data of the thermal expansion coefficient α_T are 5.8,[17] 6.81,[16] 7.5,[14] 7.7–8.2,[12] and 8.2 $\times 10^{-6}$/K.[13] We use the value published by Wynne *et al.*[16] because it is close to the average value of available data and includes values of the temperature-dependent data. Published data of the change in refractive index with temperature are, at room temperature, 9.0,[16] 7.3,[12] 8.3,[14] and 9.86 $\times 10^{-6}$/K.[15] We use the average value of Refs. 14 and 16 because these references provide temperature-dependent data from which we calculate the value of the almost linear increase of dn_o/dT with temperature of $d^2n_o/dT^2 = 2.6 \times 10^{-8}/K^2$. The other parameters used in the calculation are $n_o = 1.82$, $\alpha = 7/\text{cm}$, $\nu = 0.28$,[12] $C_r = 0.017$,[12] $\omega_o = 0.38\,\text{mm}$, $d_1 = 0.5\,\text{cm}$, $d_2 = 19.5\,\text{cm}$, and $\rho_1 = 100\,\text{cm}$. Note that the accuracy in determining thermal loading was limited by the measurement of the critical pump power, the uncertainties in the values of the model parameters, and the error introduced by the fact that a temperature-independent thermal conductivity was used. The systematic error is estimated to be ±18% of the value of the fractional thermal loading. It is seen that the fractional thermal loading for $\omega_p/\omega_o = 1.0$ is quite close to the quantum defect, 0.24, but it increases significantly to ~0.35 for $\omega_p/\omega_o = 1.6$. In other words, there is no room for any significant physical con-

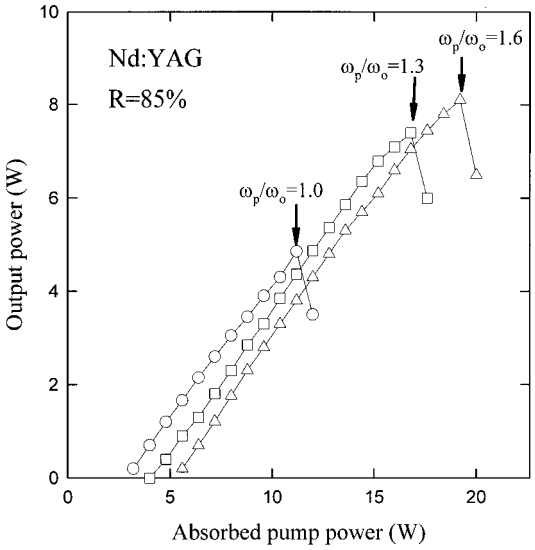

Fig. 2. Experimentally measured variation of output power as a function of absorbed pump power for several pump-to-mode size ratios.

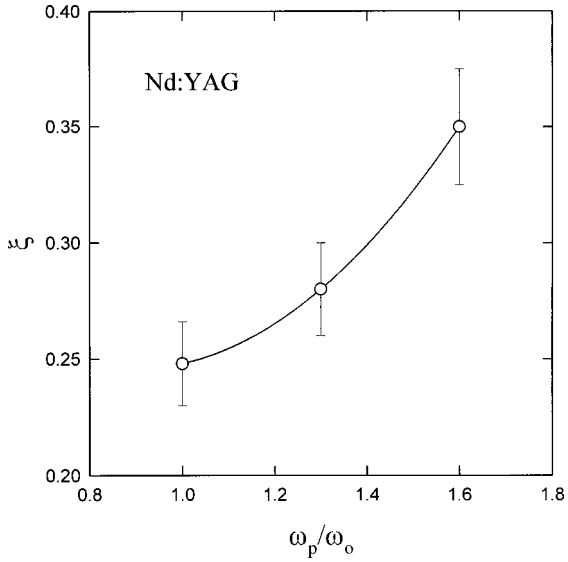

Fig. 3. Experimental results for the relationship between fractional thermal loading and the pump-to-mode size ratio.

tribution to thermal loading beyond the quantum defect in cw diode-pumped 1.0%-doped Nd:YAG lasers with $\omega_p/\omega_o = 1.0$. When $\omega_p/\omega_o = 1.6$, however, there is a significant physical contribution to thermal loading beyond the quantum defect.

Factors that contribute to thermal loading in Nd-doped crystals have been discussed widely. The thermal loading has been attributed mainly to the quantum defect, cross relaxation, impurity quenching, and nonradiative relaxation.[4] A number of papers[8,18–22] have shown that ETU has a significant influence on the thermal loading of the laser crystals. To explain the present result reasonably, we find that the ETU effect must be taken into account.

The laser field stimulates the inversion population primarily over the region within the laser mode size. Outside this region, the inversion density is seldom stimulated and continues to increase as the pumping rate is increased. Therefore the fraction of stimulated emission is lower for large pump-to-mode size ratios than for smaller ratios. If ETU were not significant, as was pointed out by Brown,[3] at 1.0–1.1 at. % for a Nd:YAG crystal the difference in heat fractions between no stimulated emission and strong saturation is only approximately 6–14%. However, recent experimental results[23,24] show that the difference in heat fractions between lasing and nonlasing cases exceeds 60% in diode-end-pumped Nd:YAG and Nd:YVO_4 crystals. In the present result the difference in heat fractions between $\omega_p/\omega_o = 1.0$ and $\omega_p/\omega_o = 1.6$ conditions is found to be ~45%. It is thus not likely that ETU represents a negligible effect in the heat generation of diode-pumped Nd-doped lasers with large pump-to-mode size ratios or without stimulated emission. In the analysis below, we can obtain a reasonable explanation by taking account of the ETU effect.

3. ANALYSIS AND DISCUSSION

The ETU process involves two nearby ions in the metastable level $^4F_{3/2}$. One ion returns to the $^4I_{9/2}$, $^4I_{11/2}$, or $^4I_{13/2}$ level by transferring its energy to the other ion, which is, in turn, brought into a higher excited state. Hardman *et al.*[8] reported that the ETU effect leads to a notable difference in the thermal lens between lasing and nonlasing conditions for a diode-end-pumped Nd:YLF laser. Hardman *et al.*[8] assumed that the inversion population density is related to the critical inversion density at the threshold condition and derived the following fractional thermal loading:

$$\xi = \frac{P_{\text{th}}}{P_{\text{abs}}}F(\beta) + \left[1 - \frac{P_{\text{th}}}{P_{\text{abs}}}F(\beta)\right]\left(1 - \frac{\lambda_p}{\lambda_l}\right), \quad (5)$$

where

$$F(\beta) = 1 - \frac{2}{\beta}\left[2(\sqrt{1+\beta} - 1) + \ln\left(\frac{4}{\beta}\frac{\sqrt{1+\beta} - 1}{\sqrt{1+\beta} + 1}\right)\right] \quad (6)$$

is the fraction of excited Nd^{3+} ions that involve the ETU processes and

$$\beta = \frac{8\gamma\tau^2\alpha}{\pi\omega_p^2}\frac{P_{\text{th}}}{h\nu_P} \quad (7)$$

is defined as a measure of the magnitude of the effect of upconversion on the overall decay rate from the upper level, α is the absorption coefficient at the pump wavelength, P_{th} is the threshold pump power, $h\nu_p$ is the pump photon energy, τ is the emission lifetime, γ is the ETU rate, λ_l is the laser wavelength, and λ_p is the pump wavelength. Equation (5) means that the ETU effect will become insignificant, as the pump power is far above threshold. In addition, inasmuch as $F(\beta)$ is an increase of β and is regarded as the fraction of excited Nd^{3+} ions that involve ETU processes at threshold, the strategy of decreasing β to reduce the influence of ETU is proposed. From Eq. (7), expanding pump size can lead to a decrease in β and then a reduction in thermal loading. Nevertheless, this conclusion contradicts the experimental results described in Section 2. Note that we have derived Eqs. (5)–(7) by assuming that the inversion population density is equal to the critical inversion density at the threshold condition. However, the inversion population density above threshold in a cw laser is not always constant, except when $\omega_p/\omega_o \to 0$.[18] Therefore it is not correct to regard the term $F(\beta)P_{\text{th}}/P_{\text{abs}}$ in Eq. (5) as the fraction of excited Nd^{3+} ions involving ETU processes above threshold. As a consequence, Eq. (5) is not appropriate for the expression of thermal loading.

As reported by Risk,[25] when the pump size is slightly larger than the mode size, i.e., $\omega_p/\omega_o > 1$, the total population inversion continues to increase as the pumping rate is increased above the threshold value. The pump-to-mode size ratio, ω_p/ω_o, is practically designed to be in the range of 1–1.6 for pump power greater than 3 W to prevent thermally induced diffraction losses. Because the ETU process essentially depends on the inversion population density, the influence of ETU on the thermal loading of a high-power end-pumped cw laser should depend on the pump-to-mode size ratio.

Here we use a space-dependent rate-equation analysis to consider the influence of ETU on a cw laser. For a single transverse mode and an ideal four-level laser, we can write the rate equation as[26,27]

$$\frac{dn(x,y,z)}{dt} = R_p r_p(x,y,z) - c\sigma n(x,y,z)\Phi\phi_o(x,y,z) - \frac{n(x,y,z)}{\tau} - \gamma n(x,y,z)^2, \quad (8)$$

$$\frac{d\Phi}{dt} = c\sigma\Phi\int_{\text{rod}} n(x,y,z)\phi_o(x,y,z)dV - \frac{\Phi}{\tau_c}, \quad (9)$$

where n is the upper-state population density, σ is the stimulated-emission cross section, c is the speed of light in the medium, Φ is the cavity photon number, and

$$\tau_c = \frac{2l_{\text{eff}}}{c}\frac{1}{L + \ln(1/R)} \quad (10)$$

is the photon lifetime, where $l_{\text{eff}} = l_{\text{cav}} + (n_o - 1)l$ is the effective length of the resonator, l_{cav} is the length of the

laser cavity, L is the round-trip loss, and R is the output reflectivity. R_p is the pumping rate and is given by

$$R_p = \frac{P_{\text{abs}}}{h\nu_p}. \tag{11}$$

The main difference between the present and previous models[26,27] is that, in the former, $\gamma n(x, y, z)^2$ was added to Eq. (8) to take the ETU effect into account. The functions $r_p(x, y, z)$ and $\phi_o(x, y, z)$ describe the spatial variation of the pump beam and the fundamental laser cavity mode, respectively. These terms are normalized such that

$$\int_{\text{rod}} r_p(x, y, z)\mathrm{d}V = \int_{\text{cavity}} \phi_o(x, y, z)\mathrm{d}V = 1. \tag{12}$$

The beam profile of a fiber-coupled laser diode can be approximately described as a top-hat distribution[28,29]:

$$r_p(x, y, z) = \frac{1}{\pi\omega_p{}^2}\frac{\alpha\exp(-\alpha z)}{1-\exp(-\alpha l)}\Theta(\omega_p{}^2 - x^2 - y^2), \tag{13}$$

where $\Theta(\,)$ is the Heaviside step function. For a single transverse mode, TEM_{00}, $\phi_o(x, y, z)$ is given by

$$\phi_o(x, y, z) = \frac{2}{\pi\omega_l{}^2(z)l_{\text{eff}}}\exp\left[-2\frac{x^2+y^2}{\omega_l{}^2(z)}\right], \tag{14}$$

$$\omega_l(z) = \omega_o\{1 + [(z - z_l)\lambda_1/\pi\omega_o{}^2]^2\}^{1/2} \approx \omega_o\,. \tag{15}$$

Here z_l is the position of the beam waist and the point $z = 0$ is taken to be the incident surface of the active medium.

In the steady state, $\mathrm{d}n/\mathrm{d}t = 0$, and the general expression for $n(x, y, z)$ derived from Eq. (8) is given by

$$n(x, y, z) = \frac{2R_p r_p(x, y, z)}{\left[\frac{1}{\tau} + c\sigma\Phi\phi_o(x, y, z)\right] + \left\{\left[\frac{1}{\tau} + c\sigma\Phi\phi_o(x, y, z)\right]^2 + 4\gamma R_p r_p(x, y, z)\right\}^{1/2}}. \tag{16}$$

Before determining $n(x, y, z)$ as a function of the pumping rate, we need to find the relationship between pumping rate R_p and cavity photon number Φ. Substituting Eq. (16) into Eq. (9) and using $\mathrm{d}\Phi/\mathrm{d}t = 0$ yield the relationship between the pumping power and the cavity photon number Φ:

$$\int_{\text{rod}} \frac{2\phi_o(x, y, z)r_p(x, y, z)}{1 + c\sigma\tau\Phi\phi_o(x, y, z) + \left\{[1 + c\sigma\tau\Phi\phi_o(x, y, z)]^2 + \frac{4\gamma\tau^2 P_{\text{abs}}}{h\nu_p}r_p(x, y, z)\right\}^{1/2}}\mathrm{d}V = \left(\frac{P_{\text{abs}}}{P_{\text{th},o}}\right)^{-1}\int_{\text{rod}}\phi_0 r_p\mathrm{d}V. \tag{17}$$

where

$$P_{\text{th},o} = \frac{\ln(1/R) + L}{2l_{\text{eff}}}\frac{h\nu_p}{\sigma\tau}\frac{1}{\int_{\text{rod}}\phi_o r_p\mathrm{d}V} \tag{18}$$

is the threshold without the ETU effect.

With the relationship between the pumping power and the cavity photon number, we find the total population number by integrating the population density over the crystal volume:

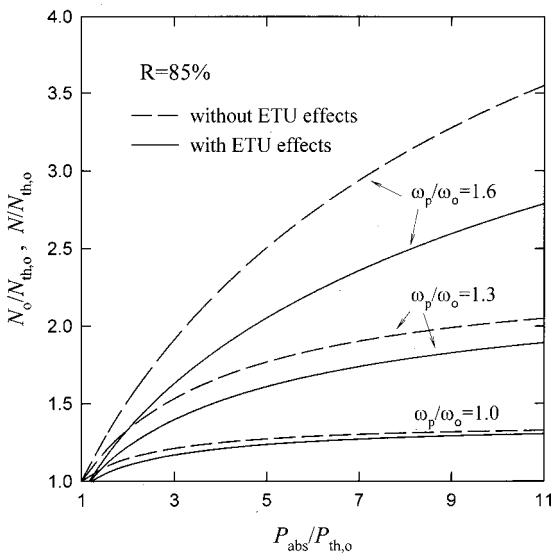

Fig. 4. Numerical calculations of $N/N_{\text{th},o}$ and $N_o/N_{\text{th},o}$ as a function of $P_{\text{abs}}/P_{\text{th},o}$ for several values of the pump-to-mode size ratio.

$$N = \int_{\text{rod}} n(x, y, z)\mathrm{d}V. \tag{19}$$

If $\gamma = 0$, i.e., if there are no ETU effects, the total population number is given by

$$\frac{N_o}{N_{\text{th},o}} = \frac{P_{\text{abs}}}{P_{\text{th},o}}\int_{\text{rod}}\frac{r_p(x, y, z)}{1 + c\sigma\tau\Phi\phi_o(x, y, z)}\mathrm{d}V, \tag{20}$$

where $N_{\text{th},o} = P_{\text{th},o}\tau/h\nu_p$ is the total population number at threshold without ETU effects. Similarly, Φ needs to be solved from

$$\int_{\text{rod}}\frac{\phi_o(x, y, z)r_p(x, y, z)}{1 + c\sigma\tau\Phi\phi_o(x, y, z)}\mathrm{d}V = \left(\frac{P_{\text{abs}}}{P_{\text{th},o}}\right)^{-1}\int_{\text{rod}}\phi_0 r_p\mathrm{d}V. \tag{21}$$

To illustrate that the total inversion above threshold depends critically on the value of ω_p/ω_o, we use expressions (13)–(19) and the following parameters: $\sigma = 2.8 \times 10^{-19}\,\text{cm}^2$,[12] $\gamma = 2.8 \times 10^{-16}\,\text{cm}^3/\text{s}$,[18] $\alpha = 7\,\text{cm}^{-1}$, $\omega_o = 0.38\,\text{mm}$, $L = 0.006$, $R = 0.85$, and $\tau = 230\,\mu\text{s}$, to

calculate N. Figure 4 depicts $N/N_{\mathrm{th},o}$ as a function of the ratio of the absorbed pump power to the threshold without ETU effects, $P_{\mathrm{abs}}/P_{\mathrm{th},o}$, for various values of the pump-to-mode size ratio. The ratio $N_o/N_{\mathrm{th},o}$ is also plotted in the same figure to show the influence of ETU effects on population inversion. It can be seen that the total inversion initially continues to increase as the pumping rate is increased above the threshold value. As the pumping rate is intense enough to saturate the gain distribution over the entire pumping region, $N/N_{\mathrm{th},o}$ saturates to a much larger value for a larger ω_p/ω_o, and so does $N_o/N_{\mathrm{th},o}$. The difference between $N/N_{\mathrm{th},o}$ and $N_o/N_{\mathrm{th},o}$, however, represents the fractional reduction of the population inversion that is due to ETU effects. Figure 4 shows that the larger the pump-to-mode size ratio is, the more significant is the population reduction that is due to ETU effects in an end-pumped cw laser. In other words, as the pump size is increased for a given mode size, the fraction of excited ions involving ETU processes is increased. This is the reason why the thermal loading is an increasing function of the pump-to-mode size ratio.

With N_o and N, the fractional reduction of the population inversion that is due to ETU can be expressed as

$$F_{\mathrm{ETU}} = \frac{N_o - N}{N_o}. \tag{22}$$

The factor F_{ETU} represents the fraction of excited Nd^{3+} ions that involve the ETU processes. With the results shown in Fig. 4, we calculate F_{ETU} as a function of $P_{\mathrm{abs}}/P_{\mathrm{th},o}$ for several values of the pump-to-mode size ratio, as plotted in Fig. 5. As expected, F_{ETU} increases with enlargement of the pump-to-mode size ratio. Furthermore, F_{ETU} does not obviously decrease, as the pump power is far above threshold. Even when $\omega_p/\omega_o = 1.6$, F_{ETU} rapidly increases as the pumping rate is increased above the threshold value.

The heat generated from the ETU processes is due to the multiphonon relaxation from the excited level back to the upper laser level. The energy of the multiphonon relaxation is equal to the energy of the correlated downconversion transition.[8] Therefore all the possible ETU processes emit the same heat, which is equivalent to the energy of an absorbed pump photon. In terms of F_{ETU}, the heat power that is due to the ETU processes for the laser crystal that is absorbing the pump power of P_{abs} is given by $F_{\mathrm{ETU}}P_{\mathrm{abs}}$. The fraction $1 - F_{\mathrm{ETU}}$ of excited Nd^{3+} ions that decay by means the lasing process, however, results in thermal loading equal to the quantum defect. Hence the fractional thermal loading can be expressed as

$$\xi = F_{\mathrm{ETU}} + (1 - F_{\mathrm{ETU}})\left(1 - \frac{\lambda_p}{\lambda_l}\right), \tag{23}$$

where λ_l is the laser wavelength and λ_p is the pump wavelength. With the result shown in Fig. 5 and Eq. (23), we can calculate the fractional thermal loading as a function of $P_{\mathrm{abs}}/P_{\mathrm{th},o}$ for several values of the pump-to-mode size ratio, as plotted in Fig. 6. From Fig. 2 it is clear that the critical pump power is approximately 4–5 times the threshold power. With $P_{\mathrm{abs}}/P_{\mathrm{th},o} \approx 4$–5, the fractional thermal loading shown in Fig. 6 was found to be in agreement with the experimental results shown in Fig. 3. This good agreement confirms our physical analysis and validates our space-dependent rate-equation model.

Finally, it is worthwhile mentioning that, although we have treated only the result for a Nd:YAG laser, the ETU process was found to be a common effect for a Nd-doped gain medium, such as Nd:YLF,[8] Nd:YVO_4, and Nd:LSB crystals.[22] Therefore, for scaling up a cw diode-end-pumped Nd-doped crystal laser to higher power, the pump-to-mode size ratio should be designed to be lower than 1.6 to reduce the influence of ETU.

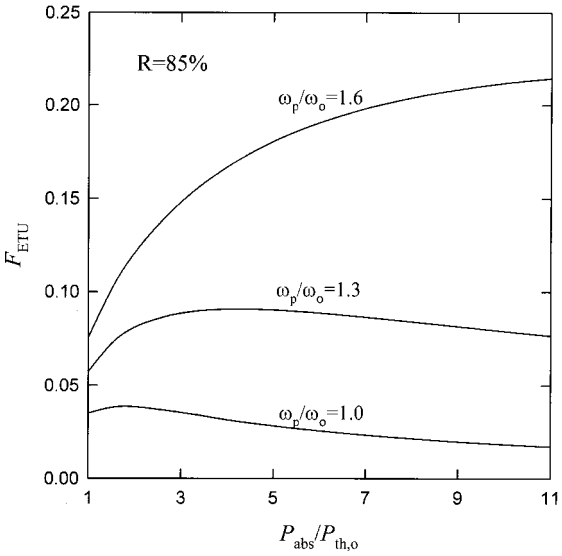

Fig. 5. Dependence of F_{ETU} on relative pumping power $P_{\mathrm{abs}}/P_{\mathrm{th},o}$ for three values of the pump-to-mode size ratio.

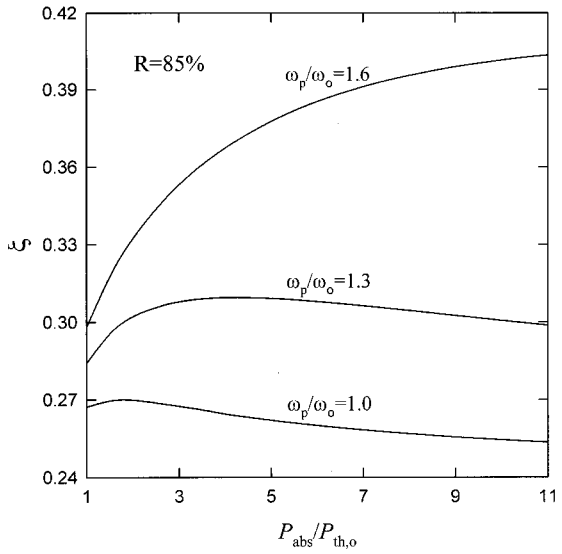

Fig. 6. Fractional thermal loading versus $P_{\mathrm{abs}}/P_{\mathrm{th},o}$ for three values of the pump-to-mode size ratio.

4. CONCLUSION

In summary, a method based on the fact that there usually exists a critical pump power at which a thermally induced focal length will cause the laser cavity to be un-

stable has been used to deduce the fractional thermal loading. Experimental results show that the fractional thermal loading is an increasing function of the pump-to-mode size ratio. The dependence of the fractional thermal loading on the pump-to-mode size ratio arises from the combined effects of the ETU processes and the unclamped behavior of the population-inversion density above threshold. A space-dependent rate-equation model that accounts for the ETU effect has been developed with which the thermal experimental data for loading in end-pumped lasers can be analyzed. The results of this model show that the pump-to-mode size ratio should be designed to be lower than 1.6 to reduce the influence of ETU in scaling up a cw diode-end-pumped Nd-doped crystal laser to higher power. This conclusion has been supported by experimental data.

ACKNOWLEDGMENT

The author thanks the National Science Council of the Republic of China for financially supporting this research under contract NSC-89-2112-M-009-059.

The author's e-mail address is yfchen@cc.nctu.edu.tw.

REFERENCES

1. B. Neuenschwander, R. Weber, and H. P. Weber, "Determination of the thermal lens in solid-state lasers with stable cavities," IEEE J. Quantum Electron. **31**, 1082–1087 (1995).
2. B. Comaskey, B. D. Moran, G. F. Albrecht, and R. J. Beach, "Characterization of the heat loading of Nd-doped YAG, YOS, YLF, and GGG excited at diode pumping wavelengths," IEEE J. Quantum Electron. **31**, 1261–1264 (1995).
3. D. C. Brown, "Heat, fluorescence, and stimulated-emission densities of fractions in Nd:YAG," IEEE J. Quantum Electron. **34**, 560–572 (1998).
4. T. Y. Fan, "Heat generation in Nd:YAG and Yb:YAG," IEEE J. Quantum Electron. **29**, 1457–1459 (1993).
5. T. S. Chen, V. L. Anderson, and O. Kahan, "Measurements of heating and energy storage in diode pumped Nd:YAG," IEEE J. Quantum Electron. **26**, 6–8 (1990).
6. B. Ozygus and J. Erhard, "Thermal lens determination of end-pumped solid-state lasers with transverse beat frequencies," Appl. Phys. Lett. **67**, 1361–1362 (1995).
7. Y. F. Chen and H. J. Kuo, "Determination of the thermal loading of diode-pumped Nd:YVO_4 by use of thermally induced second-harmonic-harmonic output depolarization," Opt. Lett. **23**, 846–848 (1998).
8. P. J. Hardman, W. A. Clarkson, G. J. Friel, M. Pollnau, and D. C. Hanna, "Energy-transfer upconversion and thermal lensing in high-power end-pumped Nd:YLF laser crystals," IEEE J. Quantum Electron. **35**, 647–655 (1999).
9. A. K. Cousins, "Temperature and thermal stress scaling in finite-length end-pumped laser rods," IEEE J. Quantum Electron. **28**, 1057–1069 (1992).
10. S. C. Tidwell, J. F. Seamans, M. S. Bowers, and A. K. Cousins, "Scaling cw diode-end-pumped Nd:YAG laser to high average powers," IEEE J. Quantum Electron. **28**, 997–1008 (1992).
11. D. Metcalf, P. De Giovanni, J. Zachorowski, and M. Leduc, "Laser resonators containing self-focusing elements," Appl. Opt. **26**, 4508–4517 (1987).
12. W. Koechner, *Solid-State Laser Engineering*, 4th ed. (Springer-Verlag, New York, 1996), p. 51.
13. C. Pfistner, R. Weber, H. P. Weber, S. Merazzi, and R. Gruber, "Thermal beam distortions in end-pumped Nd:YAG, Nd:GSGG, and Nd:YLF rods," IEEE J. Quantum Electron. **30**, 1605–1615 (1994).
14. U. Brauch, "Temperature dependence of efficiency and thermal lensing of diode-laser-pumped Nd:YAG lasers," Appl. Phys. B **58**, 397–402 (1994).
15. A. A. Kaminskii, *Laser Crystals*, Vol. 14 of Springer Series in Optical Science (Springer-Verlag, Berlin, 1981).
16. R. Wynne, J. L. Daneu, and T. Y. Fan, "Thermal coefficients of the expansion and refractive index in YAG," Appl. Opt. **38**, 3282–3285 (1999).
17. D. C. Brown, "Ultrahigh-average-power diode-pumped Nd:YAG and Yb:YAG lasers," IEEE J. Quantum Electron. **33**, 861–873 (1997).
18. Y. Guyot, H. Manan, J. Y. Rivoire, R. Moncorgé, N. Garnier, E. Descroix, M. Bon, and P. Laporte, "Excited-state-absorption and upconversion studies of Nd^{3+}-doped single crystals $Y_3A_{15}O_{12}$, $YLiF_4$, and $LaMgAl_{11}O_{19}$," Phys. Rev. B **51**, 784–799 (1995).
19. S. A. Payne, G. D. Wilke, L. K. Smith, and W. F. Krupke, "Auger upconversion losses in Nd-doped laser glasses," Opt. Commun. **111**, 263–268 (1994).
20. S. Guy, C. L. Bonner, D. P. Shepherd, D. C. Hanna, A. C. Tropper, and B. Ferrand, "High-inversion density in Nd:YAG: upconversion and bleaching," IEEE J. Quantum Electron. **34**, 900–909 (1998).
21. M. Pollnau, P. J. Hardman, W. A. Clarkson, and D. C. Hanna, "Upconversion, lifetime, quenching, and ground state bleaching," Opt. Commun. **147**, 203–211 (1998).
22. V. Ostroumov, T. Jensen, J. P. Meyn, G. Huber, and M. A. Noginov, "Study of luminescence concentration quenching and energy transfer upconversion in Nd-doped $LaSc_3(BO_3)_4$ and $GdVO_4$ laser crystals," J. Opt. Soc. Am. B **15**, 1052–1060 (1998).
23. M. Pollnau, W. A. Clarkson, and D. C. Hanna, "Thermal lensing in end-pumped Nd:YAG under lasing and nonlasing conditions," in *Conference on Lasers and Electro-Optics (CLEO/U.S.)*, Vol. 6 of 1998 OSA Technical Digest Series (Optical Society of America, 1998), pp. 100–101, paper CTUI 1.
24. J. L. Blows, T. Omatsu, J. Dawes, H. Pask, and M. Tateda, "Heat generation in Nd:YVO_4 with and without laser action," IEEE Photonics Technol. Lett. **10**, 1727–1729 (1998).
25. W. P. Risk, "Modeling of longitudinally pumped solid-state lasers exhibiting reabsorption losses," J. Opt. Soc. Am. B **5**, 1412–1423 (1988).
26. K. Kubodera and K. Otsuka, "Single-transverse-mode $LiNdP_4O_{12}$ slab waveguide laser," J. Appl. Phys. **50**, 653–658 (1979).
27. P. Laporta and M. Brussard, "Design criteria for mode size optimization in diode-pumped solid-state lasers," IEEE J. Quantum Electron. **27**, 2319–2326 (1991).
28. Y. F. Chen, T. M. Huang, C. F. Kao, C. L. Wang, and S. C. Wang, "Optimization in scaling fiber-coupled laser-diode end-pumped laser to high power: influence of thermal effect," IEEE J. Quantum Electron. **33**, 1424–1429 (1997).
29. Y. F. Chen, "Design criteria for concentration optimization in scaling diode end-pumped lasers to high powers: influence of thermal fracture," IEEE J. Quantum Electron. **35**, 234–239 (1999).